

## Article

# Anti-Aging Properties of *Cannabis sativa* Leaf Extract against UVA Irradiation

Kunlathida Luangpraditkun<sup>1</sup>, Preeyanuch Pimjuk<sup>2</sup>, Preeyawass Phimnuan<sup>3</sup>, Wisanee Wisanwattana<sup>2</sup>, Chothip Wisespongpan<sup>4</sup>, Neti Waranuch<sup>2</sup> and Jarupa Viyoch<sup>3,\*</sup>

<sup>1</sup> Research Unit of Pharmaceutical Innovations of Natural Products (PhInNat), Burapha University, Chonburi 20131, Thailand; kunlathida.lu@go.buu.ac.th

<sup>2</sup> Cosmetics and Natural Products Research Center, Faculty of Pharmaceutical Sciences, Naresuan University, Phitsanulok 65000, Thailand; preeyanuchp@nu.ac.th (P.P.); wisanee.wi@nu.ac.th (W.W.); netiw@nu.ac.th (N.W.)

<sup>3</sup> Department of Pharmaceutical Technology, Faculty of Pharmaceutical Sciences and Center of Excellence for Innovation in Chemistry, Naresuan University, Phitsanulok 65000, Thailand; p.preeyawass@gmail.com

<sup>4</sup> Institute for Small and Medium Enterprise Development (ISMED), Pathum Thani 12120, Thailand; bpd.project030@gmail.com

\* Correspondence: jarupav@nu.ac.th; Tel.: +66-55-96-18-75

**Abstract:** Hemp extract has garnered interest as a potential cosmeceutical agent with multifunctional activities, particularly in protecting against UV-induced skin cell aberrations and restoring aged skin cells. The ethanolic extract of *Cannabis sativa* leaves was prepared into an aqueous solution (CLES) to investigate its anti-photoaging ability. HPLC analysis revealed that the CLES contained  $1.64 \pm 0.01\%$  *w/w* of cannabidiol and  $0.11\%$  *w/w* of  $\Delta^9$ -tetrahydrocannabinol. Additionally, the total phenolic content was found to be  $4.08 \pm 0.30$  mg gallic acid equivalent per g of solution using the Folin–Ciocalteu method. The CLES exhibited potent scavenging activity using a DPPH assay, with an EC<sub>50</sub> value of  $277.9 \pm 2.41$   $\mu\text{g/mL}$ , comparable to L-ascorbic acid, with  $2.19 \pm 0.28$   $\mu\text{g/mL}$ . The anti-photoaging potential of the CLES was evaluated using UVA-irradiated and *in vitro*-aged fibroblasts as a model. Pre-treatment with 20  $\mu\text{g/mL}$  CLES for 24 h significantly alleviated the reduction in type I procollagen and suppressed the overproduction of MMP-1 and IL-6 induced by UVA. Moreover, the percentage of senescence-associated  $\beta$ -galactosidase-expressing cells decreased significantly to  $11.9 \pm 0.5\%$  in the aged cells treated with CLES compared with untreated cells ( $18.8 \pm 3.8\%$ ). These results strongly indicate the cosmeceutical potential of the CLES as an effective active agent for the anti-photoaging prevention and/or treatment.

**Keywords:** *Cannabis sativa*; hemp leaves extract; UVA-irradiated fibroblasts; *in vitro*-aged fibroblasts; anti-photoaging



**Citation:** Luangpraditkun, K.; Pimjuk, P.; Phimnuan, P.; Wisanwattana, W.; Wisespongpan, C.; Waranuch, N.; Viyoch, J. Anti-Aging Properties of *Cannabis sativa* Leaf Extract against UVA Irradiation. *Cosmetics* **2024**, *11*, 45. <https://doi.org/10.3390/cosmetics11020045>

Academic Editor: Enzo Berardesca

Received: 25 January 2024

Revised: 13 March 2024

Accepted: 14 March 2024

Published: 18 March 2024



**Copyright:** © 2024 by the authors. Licensee MDPI, Basel, Switzerland. This article is an open access article distributed under the terms and conditions of the Creative Commons Attribution (CC BY) license (<https://creativecommons.org/licenses/by/4.0/>).

## 1. Introduction

The skin is an organ responsible for covering and protecting our body's internal environment from external factors, including UV light, heat, and pollution. It plays a crucial role in responding to external exposures, aiming to prevent further damage to itself. For instance, after a short duration of UV exposure, the skin may exhibit redness or erythema accompanied by a burning sensation as a warning sign of inflammation. The process of UV-induced inflammation is initiated by the presence of free radicals, such as reactive oxygen species (ROS) and reactive nitrogen species (RNS), as well as oxidized molecules generated when the skin is exposed to UV rays. This oxidative stress triggers the activation of a transcriptional factor called NF- $\kappa$ B in skin fibroblasts and keratinocytes. As a result, several inflammatory cytokines, such as TNF- $\alpha$ , IL-1, and IL-6, are upregulated [1–3]. Ultraviolet (UV) exposure, especially UVA, generates free radicals that can penetrate the dermal layer of the skin. In response, skin fibroblasts are activated through the AP-1 and

MAPK signaling pathways, leading to a complex cascade of events affecting collagen metabolism. UV-induced signaling pathways influence the regulation of type I procollagen and collagenase (matrix metalloproteinase-1, MMP-1) release [4,5], with a particular focus on the role of autocrine cytokines such as IL-6 in mediating collagenase expression [6]. UV exposure induces ROS/RNS–cytokine–collagenase loop activation, leading to the upregulation of NF- $\kappa$ B/MAPK/AP-1 pathways and subsequent accumulation of aging or senescent cells in the skin. Senescence is characterized by reduced cell growth and increased SA- $\beta$ -gal activity. However, promising research has shown that the aging phenotype of fibroblasts can be partially reversed by treating cells with plant extracts or extracellular matrices derived from young fibroblasts [7,8].

In general, endogenous antioxidants play a crucial role in neutralizing free radicals generated from exposure to UV radiation [9,10]. However, chronic UV exposure can disrupt the delicate balance between oxidation and antioxidation, leading to the activation of signaling pathways responsible for skin aging via ROS/RNS activity [11–13]. Therefore, targeted skin treatments utilizing antioxidant compounds capable of suppressing ROS/RNS–cytokine–collagenase activation hold great promise in reinforcing the skin's resistance against UV damage, thereby minimizing the accumulation of aged skin cells [14–16]. Furthermore, the potential of these antioxidant substances to reverse the senescent/aged skin cells to a more youthful state presents an exciting opportunity for preventing photoaged skin.

Recently, there has been growing interest in natural extracts with multifunctional activities, particularly in their ability to protect against UV-induced skin cell aberrations and restore aged skin cells, making them promising candidates for anti-photoaging treatments. Notably, there have been reports highlighting the cosmeceutical potential of products based on *Cannabis sativa* or hemp [17,18]. The dermatopharmacological activities attributed to hemp, including antioxidation, anti-inflammation, and anti-wrinkle effects, have been closely linked to the presence of cannabinoids and phenolic compositions in hemp extract. In recent years, considerable research has been conducted on the biological activities of ethanolic extract [19] derived from hemp leaves. These activities include antioxidation, pro-MMP-2 inhibition, melanogenesis, 5 $\alpha$ -reductase inhibition, anti-bacterial activity, and anti-proliferation. However, to date, there is no existing literature on the preventive effects of *C. sativa* leaves extract on UVA-induced aberrations in human skin fibroblasts. This study aims to investigate the potential of *C. sativa* leaf extract in preventing and/or treating photoaging by assessing its impact on type I procollagen, MMP-1, and IL-6 levels in UV-irradiated fibroblasts compared to non-pretreated UV-irradiated fibroblasts. Additionally, the restoration ability of *C. sativa* leaf extract in *in vitro*-aged fibroblasts is evaluated by observing the expression of SA- $\beta$ -gal activity.

## 2. Materials and Methods

### 2.1. Preparation of the Extract Solution of *Cannabis sativa* Leaves (CLES)

The leaves of *C. sativa* (RPF3 variety) were collected from Wiang Pa Pao District, Chiang Rai Province, Thailand. The fresh leaves were thoroughly cleaned and dried at a temperature of 55–60 °C using a hot air oven. A reflux process using ethanol as the solvent was employed. The ratio of dried leaves to ethanol was maintained at 1:15 by weight at 80 °C for 2 cycles to obtain the ethanolic extract. The ethanolic extract was filtered to remove any residual particulates, and the ethanol was then evaporated using a vacuum evaporator. The evaporated paste was subsequently redissolved in the vehicle composed of a mixture of propylene glycol (food-grade, Dongying Hi-tech Spring Chemical Industry Co., Ltd., Dongying, China) and polysorbate 20 (cosmetic-grade, Croda Singapore Pte Ltd., Seraya Avenue, Singapore) in a ratio of 1:1 to obtain the *C. sativa* leaf extract solution (CLES). The obtained solution was stored in sealed packaging at 4 °C (light protection) for further investigation.

### 2.2. Determination of Cannabidiol (CBD) and Tetrahydrocannabinol (THC) Contents in the CLES

High-performance liquid chromatography (HPLC) was employed, with certain modifications from a previous study [20], to accurately determine the CBD and THC contents. The HPLC system was composed of a photodiode array detector (G7115A 1260 DAD WR detector, Agilent Technologies, Santa Clara, CA, USA) and a quaternary pump (G711A 1260 Quat pump VL, Agilent Technologies, Santa Clara, CA, USA). The standard delta-9-tetrahydrocannabinol ( $\Delta^9$ -THC) and delta-8-tetrahydrocannabinol ( $\Delta^8$ -THC) were ordered from Lipomed, Arlesheim, Switzerland and Cayman Chemical, Ann Arbor, Michigan, USA, respectively. The standard CBD was ordered from THC Pharm GmbH, Frankfurt, Germany. For the chromatographic separation, a Phenomenex C18 core-shell (150 mm  $\times$  4.6 mm, 2.6  $\mu$ m) with a column guard (C18, 4.6  $\times$  10 mm, 5.0  $\mu$ m) was employed as the stationary phase. The mobile phase comprised a mixture of acetonitrile (HPLC grade, RCI Labscan, Bangkok, Thailand) and 20 mM ammonium formate (Analytical grade, Sigma Aldrich, Steinheim, Germany) (pH 3.60) in a ratio of 75: 25% *v/v*, respectively. The column oven temperature was carefully maintained at 40 °C throughout the analysis. The mobile phase was delivered at a flow rate of 0.8 mL/min to achieve optimal chromatographic conditions. The detection of analytes was performed at a wavelength of 220 nm. The quantification of CBD and THC was achieved by creating standard curves for CBD,  $\Delta^9$ -THC, and  $\Delta^8$ -THC. The study was performed in triplicate.

### 2.3. Determination of Total Phenolic Content (TPC) of the CLES

The TPC in the CLES was determined by using the Folin–Ciocalteu method [21]. Briefly, 20  $\mu$ L of CLES was combined with 100  $\mu$ L of Folin–Ciocalteu reagent (diluted in water at a 1:10 *v/v*) and 80  $\mu$ L of sodium carbonate solution (7% *w/v* Na<sub>2</sub>CO<sub>3</sub>). The mixtures were incubated at room temperature for 30 min. Subsequently, the sample's absorbance was measured at 765 nm using a microplate reader (SpectraMax M3 UV spectrophotometer, Molecular Devices, San Jose, CA, USA). For the preparation of standards, gallic acid solution (Sigma-Aldrich, Steinheim, Germany) with a concentration in the range of 0.016–0.5 mg/mL was used. The TPC was expressed in gallic acid equivalents (mg GAE per g of CLES). All measurements were performed in triplicate.

### 2.4. Determination of Antioxidant Activity of the CLES by Using DPPH Assay

The free radical scavenging activity of the CLES was determined using the 2,2-diphenyl-1-picrylhydrazyl (DPPH) (Sigma-Aldrich, Steinheim, Germany) assay [22], and the results were compared with a positive control, L-ascorbic acid (Chem-Supply Pty Ltd., Gillman, Australia). To conduct the assay, 75  $\mu$ L of the CLES diluted in methanol or L-ascorbic acid solution was mixed with 150  $\mu$ L of 0.2 mM DPPH (Sigma-Aldrich, Steinheim, Germany) methanolic solution in a 96-well plate. Subsequently, the mixture was incubated at room temperature in the dark for 30 min. The remaining DPPH's absorbance was then measured at a wavelength of 517 nm using a microplate reader (BioStack Ready, BioTek instruments, Winooski, VT, USA). The radical scavenging activity was determined as the percentage of DPPH decoloration and calculated using the following equation:

$$\% \text{ Radical scavenging activity} = [1 - (A_S/A_B)] \times 100$$

where  $A_S$  is the absorbance of the DPPH solution without any sample and  $A_B$  is the absorbance of DPPH solution after being treated with the samples.  $EC_{50}$ , which denotes the concentration at which 50% of the desired effect is achieved, was ascertained through a log-probit analysis employing nine distinct final concentrations of the samples, with each concentration tested in triplicate.

### 2.5. Determination of Cytotoxicity of the CLES on Human Skin Fibroblasts

Normal human dermal fibroblasts (NHDFs) were purchased from Promocell (Lot no. C-12302, Eppelheim, Germany). To increase the number of NHDFs, the cells were

cultured in DMEM-high glucose (Gibco™, New York, NY, USA) containing 10% fetal bovine serum (FBS, Gibco), 1% of a stock penicillin/streptomycin solution (Gibco), and 1 mg/mL amphotericin B (Gibco) at 37 °C with a humid atmosphere containing 5% CO<sub>2</sub>. Subsequently, the cells (passage number, 5–8) were trypsinized and seeded in 96-well plates at a density of  $1.0 \times 10^4$  cells/well, then cultured in DMEM with 10% FBS and antibiotics for 24 h. Following the removal of the old medium, the cells were washed with phosphate-buffered saline (PBS), pH 7.4, and cultured in serum-free medium with or without various concentrations of CLES (10, 20, 50, 100, 500, and 1000 µg/mL) for 24 h. Cell viability was assessed using an XTT assay, and a mixture of 50 µL of the serum free-medium and 50 µL of XTT solution was added for further incubation at 37 °C in 5% CO<sub>2</sub> for 4 h. The results were measured by absorbance at 490 nm with a microplate reader (BioStack Ready, BioTek instruments, Winooski, VT, USA) to quantify the viability of the cells [23]. The viability of the non-CLES-treated NHDFs was considered as 100% viability. All experiments were performed in triplicate.

## 2.6. Determination of Preventive Effect of the CLES on UVA-Induced NHDFs Alterations

### 2.6.1. UVA Irradiation and Cell Treatment

NHDFs (passage number, 5–8) were seeded into cell culture flasks (T25) at a density of  $1 \times 10^6$  cells per flask. The cells were cultured in DMEM with 10% FBS and antibiotics at 37 °C, with a humid atmosphere containing 5% CO<sub>2</sub>, for 24 h to allow for cell adherence and growth. The adhered cells were washed with PBS and then incubated with serum-free medium without or with 20 µg/mL CLES. Following 24 h of incubation, the tested cell samples were washed and covered with a thin layer of PBS. Uniform UVA irradiation was administered using a UV test chamber BS-04 (Opsytec Dr. Gröbel GmbH, Baden-Württemberg, Germany) with a wavelength of 352 nm. The UVA intensity at the level of the culture flasks was measured using a UVA meter (Solarmeter, Solartech, Glenside, PA, USA). The distance between the samples and the lamp was maintained at 25 cm. The UVA irradiation was applied at a dosage of 5 J/cm<sup>2</sup>. After UVA irradiation, the samples were further incubated in the serum-free medium for 24 h. Subsequently, the cell-free media were then collected and stored at –80 °C for further studies. The control group consisted of the non-UVA-irradiated cells without CLES treatment. The study was performed in triplicate.

### 2.6.2. Determination of the Secreted Type I Pro-Collagen, Matrix Metalloproteinase-1 (MMP-1), and Interleukin-6 (IL-6) Levels

The commercial enzyme-linked immunosorbent assay (ELISA) kits (Human Pro-Collagen I alpha 1 ELISA Kit (ab229389, Abcam, Cambridge, UK)) and Human MMP-1 ELISA kit (ab215083, Abcam) were employed to quantify the concentration of pro-alpha1 chains of type I collagen and MMP-1 released by NHDFs into the culture medium. Furthermore, an ELISA kit (ab229434, Abcam) was employed to assess the concentration of interleukin-6 (IL-6) secreted into the culture medium by NHDFs.

## 2.7. Determination of Restoration of Aged NHDFs by the CLES

To investigate the senescence-associated β-galactosidase (SA-β-gal) activity of aged NHDFs (passage number 18–20) and NHDFs treated with CLES, a senescence detection kit (ab65351, Abcam, Cambridge, UK) was utilized. Briefly, the aged fibroblasts were seeded into a 96-well plate ( $1 \times 10^4$  cells/well) and grown in DMEM containing 10% FBS and antibiotics at 37 °C with a humid atmosphere containing 5% CO<sub>2</sub> for 24 h. The cultured cells were washed with PBS and cultured in the serum-free medium without or with 20 µg/mL CLES for 24 h. After the treatment, the tested samples were further incubated in the serum-free medium for 48 h. Following the incubation, the cells were washed with PBS and fixed with fixative solution for 15 min at room temperature, according to the manufacturer's instructions. After washing with 3X PBS, they were incubated with staining solution at 37 °C overnight. Subsequently, the stained samples were washed with

3X PBS, and the percentage of stained cells was observed under an inverted microscope. The senescent cells exhibited a characteristic blue color due to the enzymatic activity of SA- $\beta$ -gal.

### 3. Results

#### 3.1. The Appearance of the CLES and Its CBD, THC, and TPC

The ethanolic extract of *C. sativa* leaves exhibited the appearance of a green paste. For formulation, the extract was dissolved in a vehicle containing a mixture of propylene glycol and polysorbate 20 at a concentration of 19.5 g ethanolic extract per 100 g of the vehicle, resulting in a clear green solution. The HPLC assay was employed to determine the CBD and THC composition of the CLES. The analysis revealed that the CLES contained  $1.64 \pm 0.01\%$  *w/w* of CBD and  $0.11\%$  *w/w* of  $\Delta^9$ -THC. Notably, the content of  $\Delta^8$ -THC was found to be below the limit of detection (LOD), which was  $0.25 \mu\text{g/mL}$ , indicating its presence in negligible amounts. The chromatograms of the CBD and THC in the standard solution and the sample are presented in Figure 1A–C. Moreover, the TPC in the CLES was quantified using the Folin–Ciocalteu method. The results indicated a concentration of  $4.08 \pm 0.30 \text{ mg GAE per g}$  of the CLES, signifying the presence of phenolic compounds in the extract.

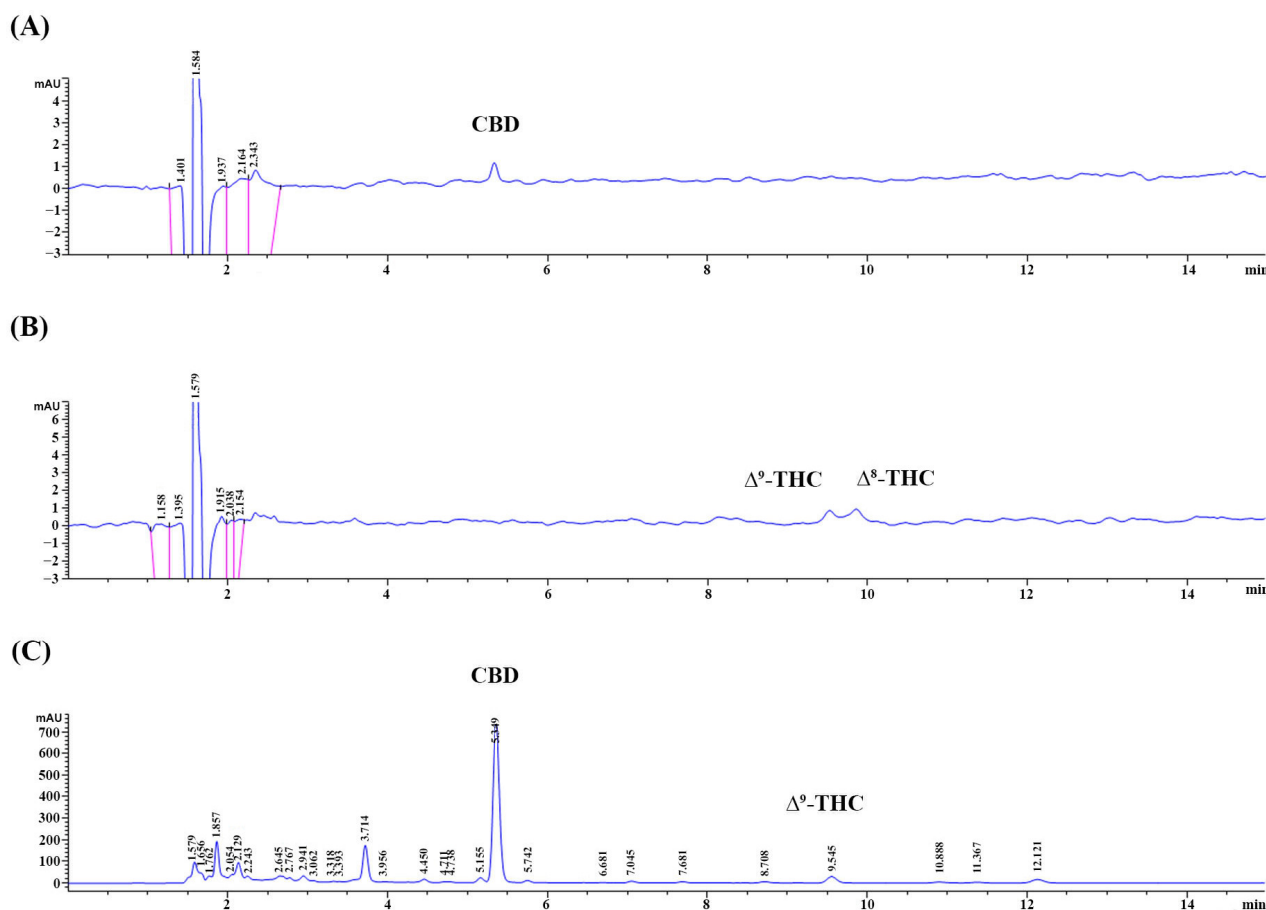


**Figure 1.** HPLC chromatograms of CBD (A) and THC (B) standard at a concentration of  $0.25 \mu\text{g/mL}$  (limit of detection, LOD) and those of CBD and THC in the CLES at a concentration of  $10 \text{ mg/mL}$  (C).

#### 3.2. Free Radical Scavenging Activity of the CLES

The DPPH assay was employed to assess the scavenging activity of the CLES and L-ascorbic acid (positive control) in a dose-dependent manner. The  $\text{EC}_{50}$  values were determined as  $277.9 \pm 2.41 \mu\text{g/mL}$  for the CLES and  $2.19 \pm 0.28 \mu\text{g/mL}$  for L-ascorbic acid.

### 3.3. Effect of the CLES on Viability of NHDFs

The cytotoxicity of CLES on NHDFs in a range of concentrations (10–1000 µg/mL) demonstrated that the viability of the cells, which was lower than 50%, was seen in the NHDFs treated with the CLES at 50 µg/mL or higher concentrations (Figure 2). However, no cytotoxicity was observed at concentrations of 20 µg/mL or lower. Furthermore, NHDFs treated with these concentrations maintained a characteristic spindle-shaped morphology typical of fibroblasts. Based on these findings, the CLES at the concentration of 20 µg/mL was selected for further studies.

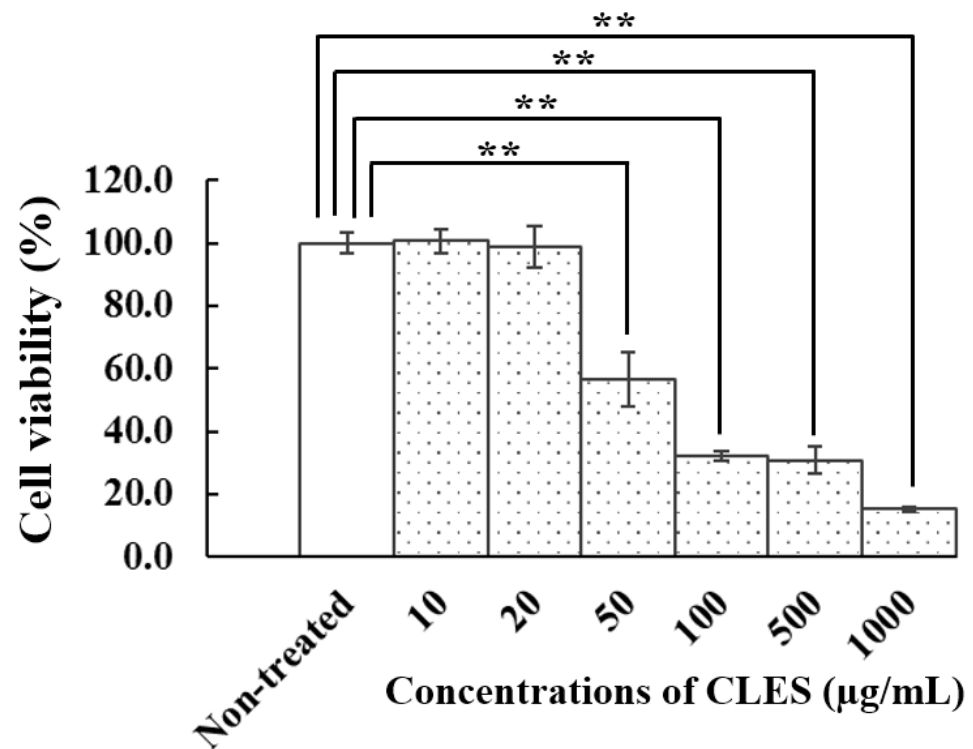


**Figure 2.** Effect of the CLES on viability of NHDFs. Cells were treated with the CLES at concentrations in the range of 10 to 1000 µg/mL for 24 h. Results are expressed as percentages of cell viability as compared to non-treated cells, for which the OD was adjusted to 100%. Each bar represents mean  $\pm$  S.D. of triplicate study. \*\*  $p < 0.01$ , when compared between two groups using unpaired Student's *t*-test.

### 3.4. Preventive Effect of the CLES on UVA-Induced Alterations of NHDFs

Following UVA exposure, a marked reduction in type I procollagen ( $p < 0.01$ ) (Figure 3A) and increased MMP-1 levels ( $p < 0.01$ ) (Figure 3B) were observed in the NHDFs' media. However, pre-treatment with 20 µg/mL CLES for 24 h significantly prevented ( $p < 0.05$ ) the reduction in type I procollagen and suppressed the overproduction of MMP-1 ( $p < 0.01$ ). Notably, the levels of type I procollagen and MMP-1 in the pre-treated group did not reach those of the control group (non-UVA-irradiated cells without CLES treatment). Furthermore, UVA-irradiated NHDFs exhibited a marked increase in IL-6 secretion ( $p < 0.01$ ) (Figure 4) compared with the control group. Nevertheless, pre-treatment with 20 µg/mL CLES significantly attenuated IL-6 overproduction ( $p < 0.05$ ).

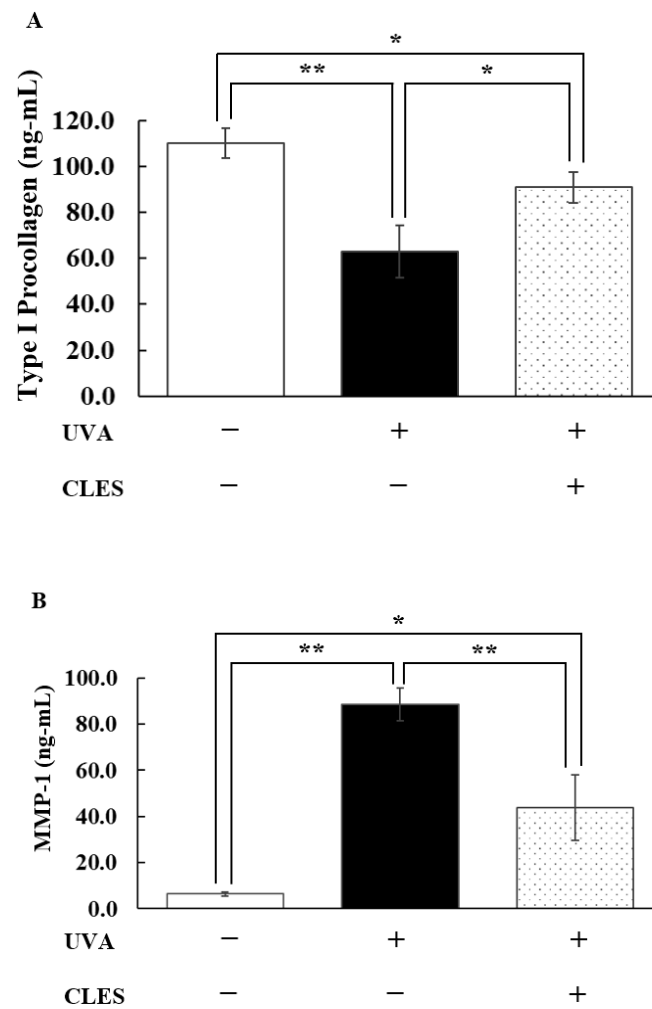


**Figure 3.** Effects of the CLES (20  $\mu\text{g}/\text{mL}$ ) on type I procollagen (**A**) and MMP-1 (**B**) secretions from UVA-irradiated NHDFs. Each bar represents mean  $\pm$  S.D. of triplicate study. \*  $p < 0.05$  and \*\*  $p < 0.01$  when compared between two groups (Student's *t*-test).

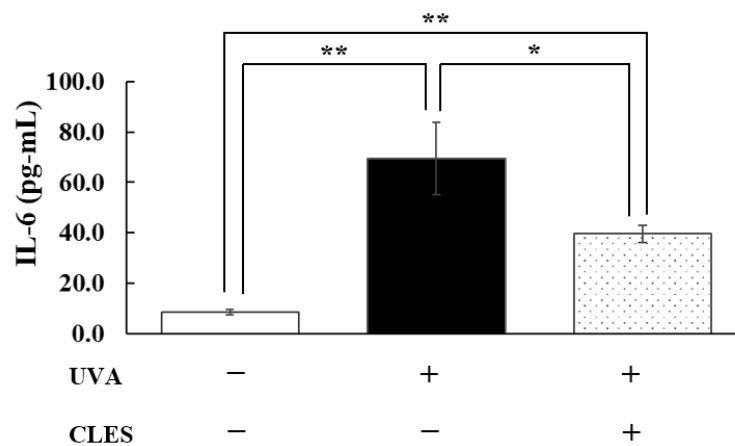


**Figure 4.** Effects of the CLES (20  $\mu\text{g}/\text{mL}$ ) on IL-6 secretion from UVA-irradiated NHDFs. Each bar represents mean  $\pm$  S.D. of triplicate study. \*  $p < 0.05$  and \*\*  $p < 0.01$  when compared between two groups (Student's *t*-test).

### 3.5. Restoration of Aged NHDFs by the CLES

Figure 5A illustrates the presence of SA- $\beta$ -gal activity in aged NHDFs (passage number 18–20), with  $18.8 \pm 3.8\%$  of the total number of cells showing positive staining. Remarkably, Figure 5B demonstrates a significant reduction ( $p < 0.05$ ) in SA- $\beta$ -gal-expressing cells ( $11.9 \pm 0.5\%$ ) with CLES treatment after 24 h compared with untreated aged cells.

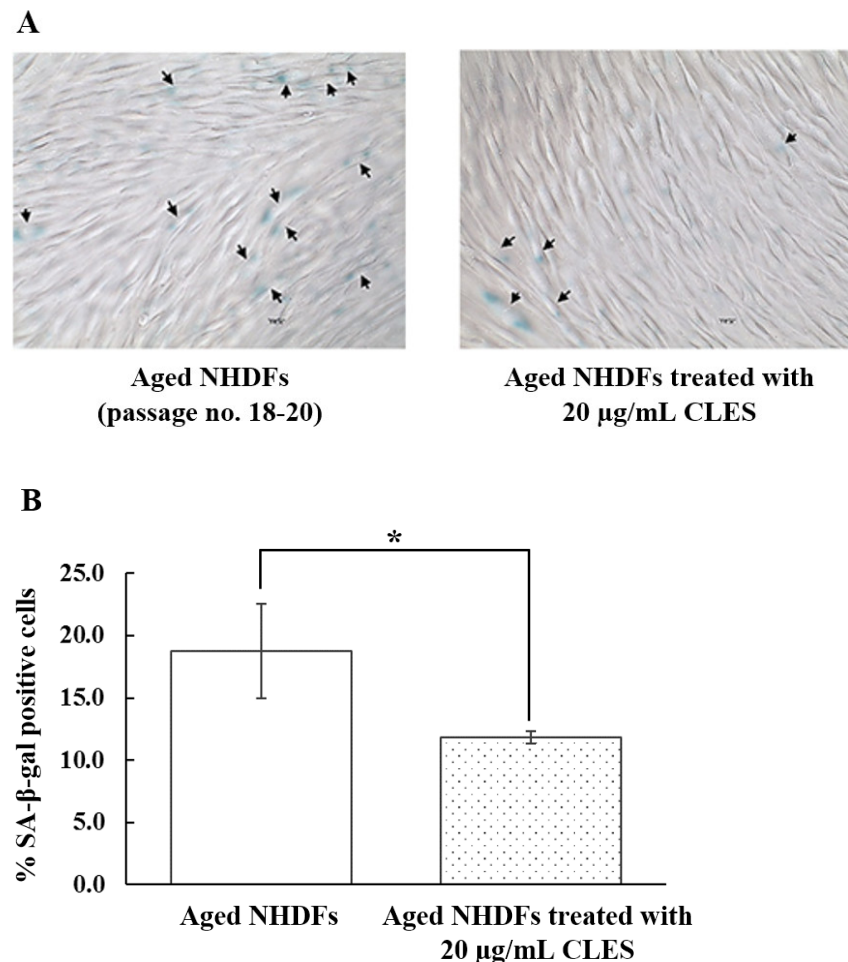


**Figure 5.** The presence of senescence-associated beta-galactosidase (SA- $\beta$ -gal) (A) and percentage of SA- $\beta$ -gal-expressing cells in the aged NHDFs and those treated with 20  $\mu\text{g}/\text{mL}$  CLES (B) is percentage of SA- $\beta$ -gal-expressing cells in the aged NHDFs and those treated with 20  $\mu\text{g}/\text{mL}$  CLES. Each bar represents mean  $\pm$  S.D. of triplicate study. \*  $p < 0.05$  when compared between two groups (Student's  $t$ -test). The arrows pointed out the SA- $\beta$ -gal-expressing cells.

## 4. Discussion

Tetrahydrocannabinol (THC) and cannabidiol (CBD) are two prominent cannabinoids found in hemp [24–26]. These compounds exhibit a range of pharmacological activities, including pain relief and anti-inflammation, but they may also lead to undesirable effects, such as anxiety and immunosuppression [27]. In hemp, the THC content is typically low, usually below 0.2% dry weight, directing the focus of dermopharmaceutical research towards CBD and other secondary metabolites, such as phenolic compounds. The therapeutic potential of hemp-based dermopharmaceuticals primarily lies in CBD and its interaction with the endocannabinoid system, which plays a vital role in skin homeostasis and health. However, the penetration of CBD into the skin without the use of enhancers is challenging due to its lipophilic nature [28]. Consequently, researchers have turned to phenolic compounds as potential skin penetration enhancers and antioxidants, which have garnered significant attention in the cosmeceutical market, particularly in products for photoaging

prevention and treatment. Among the phenolic compounds found in hemp leaves, particularly in CBD-dominant strains, are flavonoids such as orientin, vitexin, and isovitexin [29]. These flavonoids have demonstrated promising properties as antioxidants and have shown potential in enhancing skin permeation, allowing for improved dermal delivery of CBD and other beneficial compounds [30,31].

This study investigated the biological activity and composition of the ethanolic extract of hemp leaves prepared in an aqueous solution known as CLES. The aqueous form of the extract holds potential in the cosmetic market for its ease of homogenous blending into conventional cosmetic formulations, including emulsions, solutions, and gels [17,31,32]. Additionally, the solubilized form of the extract is expected to enhance the skin penetration of its active compound(s). However, the composition and biological activity of the extract solution must be investigated to ensure its beneficial effects. The composition of CLES was found to contain a small amount of CBD and THC, while its TPC was determined to be  $4.08 \pm 0.30$  mg GAE per g of CLES. The obtained contents of CBD and THC corresponded with another study [33] indicating a quite low content of THC and CBD in hemp leaves. For the content of phenols found in the CLES, this content was significant enough to exhibit *in vitro* antioxidant activity and other biological activities linked to photoaging prevention. The antioxidant activity of CLES was evaluated through DPPH assay, indicating that CLES exhibited the  $EC_{50}$  value with lower antioxidant activity ( $277.9 \pm 2.41$   $\mu\text{g}/\text{mL}$ ) than L-ascorbic acid ( $2.19 \pm 0.28$   $\mu\text{g}/\text{mL}$ ). It is well-established that L-ascorbic acid possesses remarkable antioxidant activity, which is primarily attributed to its rapid reaction with DPPH radicals. Conversely, most phenolic compounds exhibit intermediate or slow interactions with DPPH radicals. In the case of the compound CLES, its lower antioxidant activity can be attributed, at least in part, to its comparatively slow interaction with DPPH radicals [34].

For the evaluation of the biological activities of the CLES, its preventive effects on UVA-induced alterations in NHDFs were observed in cells pretreated with a concentration of 20  $\mu\text{g}/\text{mL}$  CLES. UVA radiation can penetrate the upper dermal layers and cause damage to crucial extracellular matrix (ECM) components, including collagen, elastin, and proteoglycans [35–38]. Consequently, UVA is considered a significant contributor to photoaging. Upon exposure to UVA, the skin rapidly generates free radicals, such as ROS and RNS, which directly interact with dermal components. Additionally, these free radicals can modulate fibroblast functions by activating several signaling pathways, notably NF- $\kappa$ B, MAPK, and AP-1. As a result, the expression of cytokines and matrix metalloproteinases (MMPs) increases, while the expression of type I procollagen by fibroblasts decreases [39].

In our current investigation, we observed significant changes in the expression of type I procollagen and MMP-1 in UVA-irradiated NHDFs compared with non-irradiated cells. Specifically, we noticed a considerable decrease in type I procollagen and an increase in MMP-1 expression ( $p < 0.01$ ) in the UVA-irradiated cells. These findings align with our previous study [20], providing further support to our research. Notably, when UVA-irradiated cells were pre-treated with 20  $\mu\text{g}/\text{mL}$  CLES, we observed a slight decrease in type I procollagen levels compared to non-pretreated UVA-irradiated cells. The levels of type I procollagen in the pretreated UVA-irradiated cells were significantly higher than in the non-pretreated UVA-irradiated cells ( $p < 0.05$ ). However, it is essential to highlight that the procollagen level in the pretreated UVA-irradiated cells did not reach the same level as that of non UVA-irradiated cells. Focusing on the MMP-1 and IL-6 levels, pretreatment with 20  $\mu\text{g}/\text{mL}$  CLES could significantly suppress the elevated levels of MMP-1 ( $p < 0.01$ ) and IL-6 ( $p < 0.05$ ) in UVA-exposed cells. Given the pivotal role of MMP-1 in collagen degradation within the dermis, this intervention may hold promise for preventing skin aging and related disorders. Additionally, previous research has implicated the UVA-activated NF- $\kappa$ B pathway [40] in upregulating the release of IL-6 from fibroblasts [41]. This autocrine phenomenon is linked to inflammation and an upregulation of MMP-1 expression and activation, ultimately leading to the formation of wrinkles and manifestations of photoaging. The preventive effects of CLES on UVA-activated photoaging pathways may be attributed to its potent antioxidant activity. By efficiently scavenging free radicals, the extract minimizes

the activation of downstream signaling pathways, including MAPK/AP-1/NF- $\kappa$ B/IL-6-mediated inflammation-induced aging. Additionally, the presence of phenolic compounds in the extract might activate the nuclear factor erythroid-2-related factor 2 (NRF2) signaling pathway, thus promoting the production of endogenous antioxidants and enhancing the processes that counteract aging [41,42].

Aging is a complex biological process characterized by the dysregulation of various cellular functions. In aged fibroblasts, notable changes in gene expression patterns have been observed, including significant upregulation of MMP-1, inflammatory cytokines, and biomarkers associated with senescent phenotypes. Additionally, the presence of SA- $\beta$ -gal activity is indicative of cellular aging. Interestingly, recent reports suggest the potential for restoring senescent or aged human diploid fibroblasts to a more youthful state through interaction with a young ECM [8]. Furthermore, the study observed the reversal of several senescence phenotypes, including the presence of SA- $\beta$ -gal activity. These restorative effects were attributed to specific proteins, such as Ku and SIRT1, which play crucial roles in maintaining telomere structure. In the present study, it was demonstrated that CLES has the potential to partially reverse the expression of SA- $\beta$ -gal activity in *in vitro*-aged fibroblasts. This beneficial effect of CLES may be linked to its ability to induce the expression and secretion of type I procollagen by fibroblasts. The interaction between the cells and the newly secreted ECM likely contributes to the reversal of the senescent/aged state. However, further investigations are warranted to elucidate the precise mechanisms behind the senescent reversibility of CLES. A deeper understanding of these mechanisms could have significant implications for the prevention and treatment of photoaging.

## 5. Conclusions

The extract derived from *C. sativa* leaves exhibits promising potential in preventing and/or treating photoaging. Its effects include the suppression of overproduction of MMP-1 and IL-6, while also mitigating the reduction in type I procollagen in UVA-irradiated fibroblasts. Additionally, CLES demonstrates the ability to partially reverse senescent fibroblasts by reducing the expression of SA- $\beta$ -gal activity in *in vitro*-aged fibroblasts.

**Author Contributions:** K.L. performed the experiment using a cell-based assay and analyzed and interpreted the data. P.P. (Preeyanuch Pimjuk) performed the experiment using an *in vitro* assay and analyzed and interpreted the data. P.P. (Preeyawass Phimnuan) generated and revised the manuscript. W.W. performed the HPLC experiment and analyzed and interpreted the data. C.W. prepared the extract. N.W. and J.V. designed the experiments; contributed reagents, materials, analysis tools, and data; and wrote the manuscript. All authors have read and agreed to the published version of the manuscript.

**Funding:** Financial support was obtained not only from Institute for Small and Medium Enterprise Development (ISMED), but also from Bangon Kietthanakorn, Sittisak Chuenpitayaton, Kittiya Srithanasan, and Ponsuda Poomsing (Thai-China Flavours and Fragrances Industry Co., Ltd.).

**Institutional Review Board Statement:** Not applicable.

**Informed Consent Statement:** Not applicable.

**Data Availability Statement:** The raw/processed data required to reproduce these findings cannot be shared at this time as the data also form part of an ongoing study.

**Acknowledgments:** We would like to thank the Center of Excellence for Innovation in Chemistry (PERCH-CIC), Ministry of Higher Education, Science, Research and Innovation; Global and Frontier Research University, Naresuan University: R2566C052 and R2566C053.

**Conflicts of Interest:** All authors have no conflicts of interest, and they agree to submit the manuscript to “cosmetics” as an original research article. This manuscript has not been published elsewhere and is not currently under consideration by another journal.

## References

1. Liu, S.; Mohri, S.; Manabe, Y.; Ejima, A.; Sato, K.; Sugawara, T. Gly-Pro protects normal human dermal fibroblasts from UVA-induced damages via MAPK-NF- $\kappa$ B signaling pathway. *J. Photochem. Photobiol. B* **2022**, *237*, 112601. [[CrossRef](#)]
2. Karthikeyan, R.; Kanimozhi, G.; Prasad, N.R.; Agilan, B.; Ganesan, M.; Mohana, S.; Srithar, G. 7-Hydroxycoumarin prevents UVB-induced activation of NF- $\kappa$ B and subsequent overexpression of matrix metalloproteinases and inflammatory markers in human dermal fibroblast cells. *J. Photochem. Photobiol. B* **2016**, *161*, 170–176. [[CrossRef](#)]
3. Reelfs, O.; Tyrrell, R.M.; Pourzand, C. Ultraviolet A radiation-induced immediate iron release is a key modulator of the activation of NF- $\kappa$ B in human skin fibroblasts. *J. Investig. Dermatol.* **2004**, *122*, 1440–1447. [[CrossRef](#)]
4. Yang, B.; Ji, C.; Chen, X.; Cui, L.; Bi, Z.; Wan, Y.; Xu, J. Protective effect of astragaloside IV against matrix metalloproteinase-1 expression in ultraviolet-irradiated human dermal fibroblasts. *Arch. Pharm. Res.* **2011**, *34*, 1553–1560. [[CrossRef](#)] [[PubMed](#)]
5. Quan, T.; He, T.; Voorhees, J.J.; Fisher, G.J. Ultraviolet irradiation induces Smad7 via induction of transcription factor AP-1 in human skin fibroblasts. *J. Biol. Chem.* **2005**, *280*, 8079–8085. [[CrossRef](#)] [[PubMed](#)]
6. Wlaschek, M.; Bolsen, K.; Herrmann, G.; Schwarz, A.; Wilmroth, F.; Heinrich, P.C.; Goerz, G.; Scharffetter-Kochanek, K. UVA-induced autocrine stimulation of fibroblasts-derived-collagenase by IL-6: A possible mechanism in dermal photodamage? *J. Investig. Dermatol.* **1993**, *101*, 164–168. [[CrossRef](#)]
7. Lämmermann, I.; Terlecki-Zaniewicz, L.; Weinmüllner, R.; Schosserer, M.; Dellago, H.; de Matos Branco, A.D.; Authier, D.; Sevcnikar, B.; Kleissl, L.; Berlin, I.; et al. Blocking negative effects of senescence in human skin fibroblasts with a plant extract. *N.P.J. Aging Mech. Dis.* **2018**, *11*, 4. [[CrossRef](#)] [[PubMed](#)]
8. Choi, H.R.; Cho, K.A.; Kang, H.T.; Lee, J.B.; Kaeberlein, M.; Suh, Y.; Chung, I.K.; Park, S.C. Restoration of senescent human diploid fibroblasts by modulation of the extracellular matrix. *Aging Cell* **2011**, *10*, 148–157. [[CrossRef](#)]
9. Miyachi, Y.; Imamura, S.; Niwa, Y. Decreased Skin Superoxide Dismutase Activity by a Single Exposure of Ultraviolet Radiation Is Reduced by Liposomal Superoxide Dismutase Pretreatment. *J. Investig. Dermatol.* **1987**, *89*, 111–112. [[CrossRef](#)]
10. Fuchs, J.; Huflejt, M.E.; Rothfuss, L.M.; Wilson, D.S.; Carcamo, G.; Packer, L. Impairment of Enzymic and Nonenzymic Antioxidants in Skin by UVB Irradiation. *J. Investig. Dermatol.* **1989**, *93*, 769–773. [[CrossRef](#)]
11. Steenvoorden, D.P.T.; Beijersbergen van Henegouwen, G.M.J. The use of endogenous antioxidants to improve photoprotection. *J. Photochem. Photobiol. B Biol.* **1997**, *41*, 1–10. [[CrossRef](#)]
12. Miyachi, Y. Photoaging from an oxidative standpoint. *J. Dermatol. Sci.* **1995**, *9*, 79–86. [[CrossRef](#)] [[PubMed](#)]
13. Chen, J.; Liu, Y.; Zhao, Z.; Qiu, J. Oxidative stress in the skin: Impact and related protection. *Int. J. Cosmet. Sci.* **2021**, *43*, 495–509. [[CrossRef](#)] [[PubMed](#)]
14. Varesi, A.; Chirumbolo, S.; Campagnoli, L.I.M.; Pierella, E.; Piccini, G.B.; Carrara, A.; Ricevuti, G.; Scassellati, C.; Bonvicini, C.; Pascale, A. The Role of Antioxidants in the Interplay between Oxidative Stress and Senescence. *Antioxidants* **2022**, *11*, 1224. [[CrossRef](#)]
15. Liu, X.; Xing, Y.; Yuen, M.; Yuen, T.; Yuen, H.; Peng, Q. Anti-Aging Effect and Mechanism of Proanthocyanidins Extracted from Sea buckthorn on Hydrogen Peroxide-Induced Aging Human Skin Fibroblasts. *Antioxidants* **2022**, *11*, 1900. [[CrossRef](#)] [[PubMed](#)]
16. Dunaway, S.; Odin, R.; Zhou, L.; Ji, L.; Zhang, Y.; Kadekaro, A.L. Natural Antioxidants: Multiple Mechanisms to Protect Skin from Solar Radiation. *Front. Pharmacol.* **2018**, *9*, 1–14. [[CrossRef](#)] [[PubMed](#)]
17. Zagórska-Dziok, M.; Bujak, T.; Ziemlewska, A.; Nizioł-Lukaszewska, Z. Positive effect of Cannabis sativa L. herb extracts on skin cells and assessment of cannabinoid-based hydrogels properties. *Molecules* **2021**, *26*, 802. [[CrossRef](#)]
18. Di Giacomo, V.; Recinella, L.; Chiavaroli, A.; Orlando, G.; Cataldi, A.; Rapino, M.; Di Valerio, V.; Politi, M.; Antolini, M.D.; Acquaviva, A.; et al. Metabolomic profile and antioxidant/anti-inflammatory effects of industrial hemp water extract in fibroblasts, keratinocytes and isolated mouse skin specimens. *Antioxidants* **2021**, *10*, 44. [[CrossRef](#)]
19. Manosroi, A.; Chankhampan, C.; Kietthanakorn, B.; Ruksiriwanich, W.; Chaikul, C.; Boonpisuttinant, K.; Sainakham, M.; Manosroi, W.; Tangjai, T.; Manosroi, J. Pharmaceutical and cosmeceutical biological activities of hemp (*Cannabis sativa* L. var. sativa) leaf and seed extracts. *Chiang Mai J. Sci.* **2019**, *46*, 180–195.
20. Jaidee, W.; Siridechakorn, I.; Nessopa, S.; Wisuitiprot, V.; Chaiwangrath, N.; Ingkaninan, K.; Waranuch, N. Kinetics of CBD,  $\Delta^9$ -THC degradation and cannabinol formation in cannabis Resin at various temperature and pH conditions. *Cannabis Cannabinoid Res.* **2022**, *7*, 537–547. [[CrossRef](#)]
21. Singleton, L.V.; Orthofer, R.; Lamuela-Raventó, M.R. Analysis of total phenols and other oxidation substrates and antioxidants by means of folin-ciocalteu reagent. *Methods Enzymol.* **1999**, *299*, 152–178. [[CrossRef](#)]
22. Chana, N.; Muengpoon, A.; Pethkaew, S.; Kulsin, N.; Mahasuk, A.; Srirat, S. Screening for phenolic compounds and oxidative capacity of fruit peels, agricultural waste, and traditional herbal medicine for use as biodiesel fuel additive. *Songklanakarin J. Sci. Technol.* **2022**, *44*, 1067–1074.
23. Luangpraditkun, K.; Charoensit, P.; Grandmottet, F.; Viennet, C.; Viyoch, J. Photoprotective potential of the natural artocarpin against *in vitro* UVB-induced apoptosis. *Oxid. Med. Cell Longev.* **2020**, *2020*, 1042451. [[CrossRef](#)]
24. Booz, G.W. Cannabidiol as an Emergent Therapeutic Strategy for Lessening the Impact of Inflammation on Oxidative Stress. *Free Radic. Biol. Med.* **2011**, *51*, 1054–1061. [[CrossRef](#)] [[PubMed](#)]
25. Gould, J. The Cannabis Crop. *Nature* **2015**, *525*, S2–S3. [[CrossRef](#)]
26. Kopustinskiene, D.M.; Masteikova, R.; Lazauskas, R.; Bernatoniene, J. *Cannabis Sativa* L. Bioactive Compounds and Their Protective Role in Oxidative Stress and Inflammation. *Antioxidants* **2022**, *11*, 660. [[CrossRef](#)] [[PubMed](#)]

27. Mounessa, J.S.; Siegel, J.A.; Dunnick, C.A.; Dellavalle, R.P. The role of cannabinoids in dermatology. *J. Am. Acad. Dermatol.* **2017**, *77*, 188–190. [[CrossRef](#)] [[PubMed](#)]
28. Stinchcomb, A.L.; Valiveti, S.; Hammell, D.C.; Ramsey, D.R. Human skin permeation of Delta8-tetrahydrocannabinol, cannabidiol and cannabinol. *J. Pharm. Pharmacol.* **2004**, *56*, 291–297. [[CrossRef](#)]
29. Jin, D.; Dai, K.; Xie, Z.; Chen, J. Secondary metabolites profiled in cannabis inflorescences, leaves, stem barks, and roots for medicinal purposes. *Sci. Rep.* **2020**, *10*, 3309. [[CrossRef](#)]
30. Casiraghi, A.; Musazzi, U.M.; Centin, G.; Franzè, S.; Minghetti, P. Topical administration of cannabidiol: Influence of vehicle-related aspects on skin permeation process. *Pharmaceuticals* **2020**, *13*, 337. [[CrossRef](#)]
31. Lapteva, M.; Barros, J.F.; Kalia, Y.N. Cutaneous Delivery and Biodistribution of Cannabidiol in Human Skin after Topical Application of Colloidal Formulations. *Pharmaceutics* **2024**, *16*, 202. [[CrossRef](#)]
32. Demisli, S.; Galani, E.; Goulielmaki, M.; Kyrilidis, F.L.; Ilić, T.; Hamdi, F.; Crevar, M.; Kastritis, P.L.; Pletsas, V.; Nallet, F.; et al. Encapsulation of cannabidiol in oil-in-water nanoemulsions and nanoemulsion-filled hydrogels: A structure and biological assessment study. *J. Colloid Interface Sci.* **2023**, *634*, 300–313. [[CrossRef](#)] [[PubMed](#)]
33. Knezevic, F.; Nikolai, A.; Merchart, R.; Sosa, S.; Tubaro, A.; Novak, J. Residues of herbal hemp leaf teas—How much of the cannabinoids remain? *Food Control.* **2021**, *127*, 108146. [[CrossRef](#)]
34. Sánchez-Moreno, C.; Larrauri, J.A.; Saura-Calixto, F. A procedure to measure the antiradical efficiency of polyphenols. *J. Sci. Food Agric.* **1999**, *76*, 270–276. [[CrossRef](#)]
35. Herrmann, G.; Wlaschek, M.; Lange, T.S.; Prenzel, K.; Goerz, G.; Scharffetter-Kochanek, K. UVA irradiation stimulates the synthesis of various matrix-metalloproteinases (MMPs) in cultured human fibroblasts. *Exp. Dermatol.* **1993**, *2*, 92–97. [[CrossRef](#)] [[PubMed](#)]
36. Philips, N.; Chalensouk-Khaosaat, J.; Gonzalez, S. Simulation of the Elastin and Fibrillin in Non-Irradiated or UVA Radiated Fibroblasts, and Direct Inhibition of Elastase or Matrix Metalloproteinases Activity by Nicotinamide or Its Derivatives. *J. Cosmet. Sci.* **2018**, *69*, 47–56.
37. Uitto, J. Connective tissue biochemistry of the aging dermis. Age-related alterations in collagen and elastin. *Dermatol. Clin.* **1986**, *4*, 433–446. [[CrossRef](#)]
38. Scharffetter-Kochanek, K.; Brenneisen, P.; Wenk, J.; Herrmann, G.; Ma, W.; Kuhr, L.; Meewes, C.; Wlaschek, M. Photoaging of the skin from phenotype to mechanisms. *Exp. Gerontol.* **2000**, *35*, 307–316. [[CrossRef](#)]
39. Buechner, N.; Schroeder, P.; Jakob, S.; Kunze, K.; Maresch, T.; Calles, C.; Krutmann, J.; Haendeler, J. Changes of MMP-1 and collagen type Ialpha1 by UVA, UVB and IRA are differentially regulated by Trx-1. *Exp. Gerontol.* **2008**, *43*, 633–637. [[CrossRef](#)]
40. Ding, Y.; Jiratchayamaethasakul, C.; Lee, S.H. Protocatechuic aldehyde attenuates UVA-induced photoaging in human dermal fibroblast cells by suppressing MAPKs/AP-1 and NF- $\kappa$ B signaling pathways. *Int. J. Mol. Sci.* **2020**, *21*, 4619. [[CrossRef](#)]
41. Ryšavá, A.; Čížková, K.; Franková, J.; Roubalová, L.; Ulrichová, J.; Vostálová, J.; Vrba, J.; Zálešák, B.; Svobodová, A.R. Effect of UVA radiation on the Nrf2 signalling pathway in human skin cells. *J. Photochem. Photobiol. B* **2020**, *209*, 111948. [[CrossRef](#)] [[PubMed](#)]
42. Malar, D.S.; Suryanarayanan, V.; Prasanth, M.I.; Singh, S.K.; Balamurugan, K.; Devi, K.P. Vitexin inhibits A $\beta$ 25-35 induced toxicity in Neuro-2a cells by augmenting Nrf-2/HO-1 dependent antioxidant pathway and regulating lipid homeostasis by the activation of LXR- $\alpha$ . *Toxicol. In Vitro* **2018**, *50*, 160–171. [[CrossRef](#)] [[PubMed](#)]

**Disclaimer/Publisher’s Note:** The statements, opinions and data contained in all publications are solely those of the individual author(s) and contributor(s) and not of MDPI and/or the editor(s). MDPI and/or the editor(s) disclaim responsibility for any injury to people or property resulting from any ideas, methods, instructions or products referred to in the content.